Relationship of Polymorphic Crystalline Phase Texture to Strain Recovery and Stiffness of a Propylene-Based Elastomer

P. Dias,[1]* T. Kazmierczak,[1] A. Chang,[2] P. Ansems,[2] J. Van Dun,[3] A. Hiltner,[1] E. Baer[1]

[1]*Department of Macromolecular Science and Engineering, Center for Applied Polymer Research, Case Western Reserve University, Cleveland, Ohio 44106-7202*
[2]*The Dow Chemical Company, Freeport, Texas 77459*
[3]*The Dow Chemical Company, Terneuzen, The Netherlands 4530 AA*

Received 29 August 2008; accepted 10 November 2008
DOI 10.1002/app.29823
Published online 12 March 2009 in Wiley InterScience (www.interscience.wiley.com).

ABSTRACT: A stretching process to enhance the stiffness of an elastomeric propylene-ethylene copolymer through orientation was examined. The tensile extension was performed at various temperatures within the unusually broad melting range of the copolymer. Stretching transformed the unmelted lamellar crystals into shish-kebab fibers that acted as a scaffold for an elastomeric matrix of entangled, amorphous chains. Density measurements indicated that the process did not significantly affect the amount of crystallinity, which was about 23%. If the specimen was recrystallized by cooling after it recovered from the stretched state, the amount of orientation decreased with increasing stretching temperature. However, if recrystallization occurred in the stretched state, it led to the formation of a second crystalline network that prevented contraction of the oriented crystalline structure during strain recovery. It was suggested that the second network was anchored by α'-PP daughter lamellae that crystallized epitaxially on the α-PP mother crystals of the extended fibrils. Although the manner in which the films were stretched and recrystallized strongly affected the modulus, good elasticity of the stretched films revealed the persistence of an elastomeric network. © 2009 Wiley Periodicals, Inc. J Appl Polym Sci 112: 3736–3747, 2009

Key words: polyolefin; elastomer; fibers

INTRODUCTION

Thermoplastic elastomers are a class of materials that can be processed and recycled like thermoplastics, but exhibit the physical properties of vulcanized rubbers, such as low initial modulus, uniform deformation and high recovery from large strains. Unlike vulcanized rubbers, where elasticity is derived from an amorphous network interconnected by chemical crosslinks, thermoplastic elastomers possess physical crosslinks. Commercially important thermoplastic elastomers such as segmented polyurethanes and styrenic elastomers possess a blocky chain structure consisting of higher and lower glass transition (T_g) segments. Phase separation of the higher T_g blocks creates the physical junctions that give these thermoplastic elastomers their rubbery behavior.[1,2] Polyolefin-based thermoplastic elastomers have received considerable attention because of their chemical inertness, low density, and low cost compared with other TPEs.[1] In this case, a network of rubbery, amorphous polymer chain segments is anchored by crystals. The crystallizable chain segments in olefin-based TPEs are usually polyethylene or polypropylene sequences.[3–6]

We recently described the elastic behavior of a propylene-ethylene (P/E) copolymer with low crystallinity.[7,8] It was found that an initial "conditioning" tensile extension up to 800% strain resulted in an elastomer with low initial modulus, strong strain hardening, and complete recovery over many cycles. Conditioning transformed crystalline lamellae into shish-kebab fibers by melting and recrystallization. The small concentration of shish-kebab fibers acted as a scaffold for an elastomeric matrix of entangled, amorphous chains. Because the entanglement network was anchored to the relatively robust crystalline scaffold, strain recovery was virtually complete and almost instantaneous over many cycles. The major features of the model have since been supported by recently published observations on a similar P/E copolymer.[9]

The propylene-ethylene elastomers can be processed into stiff elastic fibers, nonwoven fabrics, and oriented tapes. In these processes, the polymer melt

Correspondence to: A. Hiltner (pah6@case.edu).
**Present address:* The Dow Chemical Company.
Contract grant sponsors: The Dow Chemical Company, Freeport, Texas 77459.

is extruded vertically into an open-air chamber that cools it to a few degrees above the melting temperature before it is rapidly drawn or spun. The resulting product is a highly oriented fiber or agglomeration of fibers that have chain axis orientation. The crystallographic and amorphous chain orientations have been probed extensively, most notably with synchrotron beam lines in conjunction with a drawing apparatus.[10–12] Because cooling and stretching of the partially melted polymer occur simultaneously, temperature effects are not decoupled from rate and draw-ratio effects. The problem is aggravated by the inherently narrow melting range of commercially available polypropylene copolymers.

In this study, we probe the effect of process temperature on the crystalline scaffold in a P/E copolymer by performing the initial conditioning tensile extension at various temperatures within the broad melting range of the copolymer. The order in which recrystallization and recovery are performed is reversed by cooling either before or after the load is removed. The effect on the resulting elastomeric properties, such as modulus and strain recovery, is examined.

MATERIALS AND METHODS

The propylene-ethylene copolymer used in this study was supplied by The Dow Chemical Company. It was prepared with a postmetallocene catalyst. It contained 17 mol % ethylene and is designated as P/E17. The crystallinity was 21 wt % from density. The weight average molecular weight M_w was 1.4×10^5 g mol^{-1} as determined by gel permeation chromatography calibrated with polystyrene standards. The equivalent polypropylene molecular weights were deduced using appropriate Mark-Houwink coefficients for polypropylene and polystyrene.

The melting behavior of P/E17 was determined using a Perkin–Elmer Model 7 DSC. The sample was cooled from the melt at 10°C min^{-1} to −30°C prior to the second heating. The onset of melting occurred below ambient temperature and ended at ~ 143°C.

Films 0.5-mm thick were compression molded from pellets into plaques as described previously.[8] The plaques were aged for 7 to 12 days under ambient conditions before further testing. Microtensile specimens were cut from the plaques according to ASTM 1708 and uniaxially stretched with an MTS Alliance RT/30 electromechanical testing machine. The stretching temperature was controlled by using an Instron model 3119-009 environmental chamber. The crosshead speed for all specimens was 22.3 mm min^{-1} which was 100% min^{-1} for the initial microtensile specimen geometry.

The microtensile specimens were stretched to a target strain of 600% at 20°C (ambient temperature), 30, 40, 50, 55, 60, and 70°C. Stretched specimens were cooled in one of two ways. In one case, the load was removed at the stretch temperature, and the specimen was held at the stretching temperature for 10 min before it was cooled to ambient temperature. In this case, the specimen recrystallized after recovery as it cooled to ambient temperature. In the other case, the specimen was cooled to ambient temperature immediately after reaching 600% strain and held at this strain for 10 min before the load was removed. In this case, the specimen recrystallized before recovery while it was held in the stretched condition.

The extent to which the P/E17 films recovered after stretching was calculated as

$$\text{Recovery } (\%) = \left[1 - \frac{l_t - l_0}{l - l_0}\right] \times 100 \qquad (1)$$

where l_0 is the initial gauge length, l is the gauge length at 600% strain, and l_t is the gauge length 24 h after stretching.[13]

The density of stretched films was measured using an isopropanol-water gradient density column according to ASTM D1505-98e1. The crystallinity X_c was calculated from density assuming a two-phase model with constant amorphous phase and crystalline phase densities

$$X_c \text{ (wt\%)} = \frac{\rho_c}{\rho}\left(\frac{\rho - \rho_a}{\rho_c - \rho_a}\right) \times 100\% \qquad (2)$$

where ρ, ρ_a and ρ_c are the bulk density, amorphous phase density, and crystalline phase density, respectively. The generally accepted values of ρ_a and ρ_c for propylene of 0.853 and 0.946 g cm^{-3}, respectively,[14,15] were used in the calculation.

The stress-strain behavior of the stretched films was measured 24 h after the stretching process. The specimens were loaded at 100% min^{-1} with stress and strain based on the new gauge length. The secant modulus at 30% strain was taken from the stress-strain curve. The strain recovery after the specimen was loaded to 30% strain and released from the grips was measured.

Wide angle X-ray scattering (WAXS) was used to characterize the crystalline phase. The 2D WAXS patterns were obtained using CuK_α radiation with a Philips PW 1830 generator operating at 30 kV and 35 mA. The patterns were recorded on Fujifilm image plates with an exposure of 8 h. A Fujifilm IP FDL 5000 reader was used to process the images. To determine the relative amounts of α-PP and γ-PP, the stretched films were cryogenically ground and the 1D WAXS diffractograms were obtained using CuK_α radiation with a Rigaku RING 2200 Ultima with a 2θ angle range of 10–35°, in 0.05° increments and a sampling speed 0.2°/min.

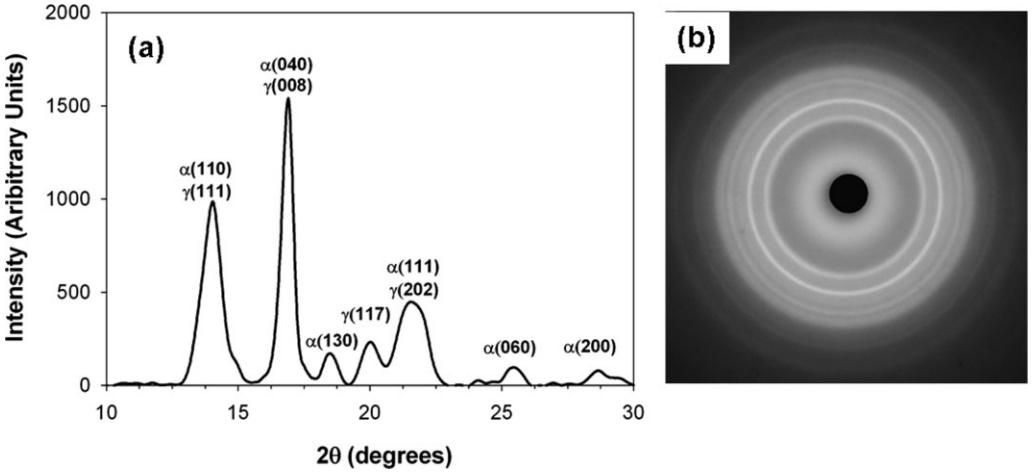

Figure 1 X-ray diffraction from unstretched, compression molded PE/17: (a) 1D WAXS diffractogram; and (b) 2D WAXS pattern.

Atomic force microscopy (AFM) was performed on unoriented controls and conditioned specimens. Specimens for AFM were stretched at 20°C or at 50°C and cooled to 20°C before being placed in the AFM. Specimens were imaged in a Digital Instruments Nanoscope IIIa using a special specimen holder to maintain the stretched state. Before imaging, the specimens were acid etched for 3 min using a 1 : 2 (vol : vol) solution of sulfuric acid : orthophosphoric acid with 0.7 wt % potassium permanganate.[16]

RESULTS AND DISCUSSION

The crystalline phase of P/E17 consisted of both alpha (monoclinic) and gamma (orthorhombic) modifications of isotactic polypropylene (iPP). The diffractogram of the unoriented P/E17 is shown in Figure 1(a) with the amorphous halo subtracted. The isotropic rings in the 2D WAXS pattern confirm that the crystalline phase is not oriented, Figure 1(b). The peaks appear at 2θ of 14.1° which corresponds to α-PP (110) and γ-PP (111), at 16.7° which corresponds to α-PP (040) and γ-PP (008), and at 21.1° which corresponds to α-PP (111) and γ-PP (202).[17–19] The peaks for γ-PP overlap with those of the α-PP at many Bragg angles. Fortunately, there are two peaks in which the γ-PP and α-PP do not overlap. The strong reflection of the α-form at 18.6 (130) is absent in the γ-form, and a reflection appears at 20.1° for γ-PP (117) which is absent in the α-form. The ratio of the α-PP (130) peak intensity to the γ-PP (117) peak intensity can be used to calculate the relative contribution of each form to the total crystallinity. The volume fraction γ-PP in the crystalline phase of a specimen containing both α-PP and γ-PP can be obtained as

$$K_\gamma = \frac{I_\gamma(117)}{I_\gamma(117) + I_\alpha(130)} \tag{3}$$

where $I_\gamma(117)$ and $I_\alpha(130)$ denote intensities of the (117) and (130) deconvoluted diffraction peaks of γ-PP and α-PP, respectively.[20,21] The experimental diffractograms were deconvoluted after subtraction of the background, and the undeformed control film was found to have ~ 70% of its crystallinity as γ-PP, and the remainder as α-PP. The total crystallinity calculated from the density was 21 wt %.

The AFM height and phase images of an etched P/E17 surface are shown in Figure 2(a,b), respectively. The images show randomly oriented lamellae with conspicuous cross-hatching, that is, smaller lamellae growing epitaxially and almost perpendicularly on larger lamellar spines. Because γ-PP is known to grow on α-PP, and that the reverse is prohibited,[22–24] it is most probable that the α-PP forms the spines, and that the epitaxy, which makes up the majority of the crystalline material, is γ-PP.

Stretching at ambient temperature

Three protocols were used to stretch the P/E film: (1) The film was stretched to 600% at ambient temperature (20°C) and recovered at the same temperature, Figure 3(a); (2) the film was stretched to 600% at an elevated temperature, and the load was removed at the stretch temperature so that the specimen recovered before it recrystallized during cooling to 20°C, Figure 3(b), and (3) the film was stretched to 600% at an elevated temperature and was held at 600% strain during cooling to 20°C, so that it recrystallized in the stretched condition, after which the load was removed, Figure 3(c). The resulting

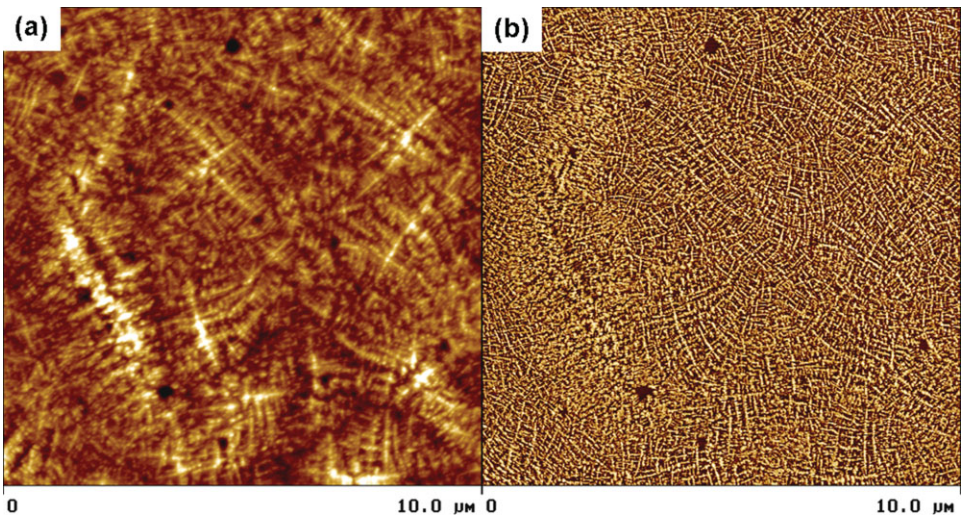

Figure 2 AFM images of unstretched, compression molded P/E17: (a) Height image; and (b) phase image. [Color figure can be viewed in the online issue, which is available at www.interscience.wiley.com.]

specimens were characterized 24 h after stretching. The stretching protocol did not have much effect on the final crystallinity as measured by density, and indeed the changes were often within the uncertainty in the measurement. The measured crystallinity increased only slightly from 23 wt % for the unoriented P/E film to 24–26% for the stretched films.[25]

The deformation at 20°C was typical of a P/E elastomer, featuring a low initial modulus of 6 MPa, uniform deformation, and high strain recovery after fracture. This is shown as the solid line in Figure 4. About 70% of the applied strain was recovered after stretching at 20°C. The specimen was then reloaded and the resulting stress-strain curve is shown as a dashed line in Figure 4. The stretching process imparted a dramatic increase in the modulus from 6 to 24 MPa. The shape of the curve resembled that of a melt-spun fiber.[25]

The WAXS diffractogram showed only reflections corresponding to α-PP. All reflections from γ-PP completely disappeared, indicating a complete conversion of the γ-PP crystals into α-PP crystals. The 2D WAXS pattern captured in the stretched state at 600% strain, Figure 5(a), resembled the pattern of a highly-oriented polypropylene fiber with predominantly c-axis orientation as indicated by intense equatorial spot reflections for the (110), (040), and (130) planes of the α-PP. On recovery, the spots changed to well-defined arcs with maxima on the

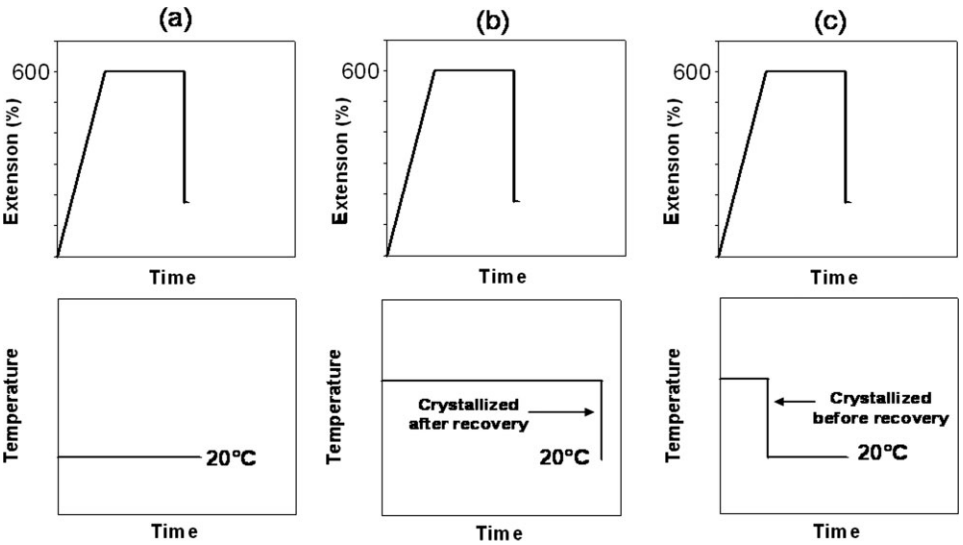

Figure 3 Extension/temperature profiles for stretching of P/E17: (a) Stretching at 20°C; (b) stretching at elevated temperature and recrystallization by cooling after recovery; and (c) stretching at elevated temperature and recrystallization by cooling before recovery.

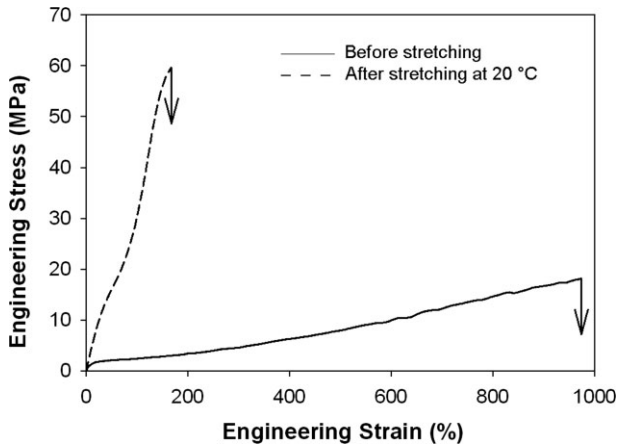

Figure 4 Stress–strain curves of P/E17: (a) unstretched (solid line); and (b) after stretching at 20°C (dashed line).

equator indicating that some orientation was lost upon strain recovery, Figure 5(b). The WAXS pattern of the recovered specimen also showed meridional reflections that were present but much weaker in the stretched condition. These corresponded to α′-PP (110) which is known to grow epitaxially on oriented α-PP crystals.[26,27] The angle between the c-axes of the α-PP and α′-PP has been reported as 80.7°.[55] The broad meridional reflection combined the two α′-PP reflections at ± 80.7°.

Direct AFM images confirmed the fiber structure inferred from 2D WAXS. Figure 6(a) shows a specimen that was imaged in the stretched state at 600% strain. The image shows thick, highly oriented fibrils oriented in the stretching direction. Figure 6(b) shows a specimen that was imaged after recovery from 600% strain. The image shows that the fibrillar structure remained after the stress was released although some orientation was lost during recovery. The thick fibrillar structure seen in Figure 6(a) became wavy and disordered in Figure 6(b). These observations were consistent with the 2D WAXS results.

A description of the structural changes that occurred during stretching and recovery of P/E17 at 20°C is based on the combined results of AFM and WAXS, Figure 7. With stretching to 600% strain, the randomly oriented lamella of α-PP and γ-PP observed in the control specimen were converted into fibrils comprising only of α-PP with a small amount of α′-PP. Upon recovery, the specimen lost some orientation although it maintained a relaxed fibrillar structure. Structural rearrangements allowed recovery of 70% of the initial strain.

Stretching at elevated temperatures with recrystallization after recovery

The P/E polymer showed an unusually broad melting endotherm, which presumably arose from a broad distribution in the crystal thicknesses. Two distinct melting regions at about 40 and 130°C were observed, Figure 8. The lower-temperature melting peak began at about 5 and ended at about 85°C. Stretching temperatures were chosen to span the low-temperature melting peak (indicated by arrows in Fig. 8) so that more of the crystals melted as the stretching temperature increased. Specimens were stretched at 30, 40, 50, 55, 60, and 70°C. Above 70°C, the polymer could not be stretched due to loss of structural integrity. Specimens drawn at 75°C fell apart at ~ 400% strain, which suggested that the crystal fractions that were responsible for holding the entanglement network together (physical cross-links) melted in this temperature range or were otherwise rendered ineffective.

For specimens that were drawn and allowed to recover at an elevated temperature before they recrystallized during cooling to 20°C, the stretching temperature had little effect on the strain recovery,

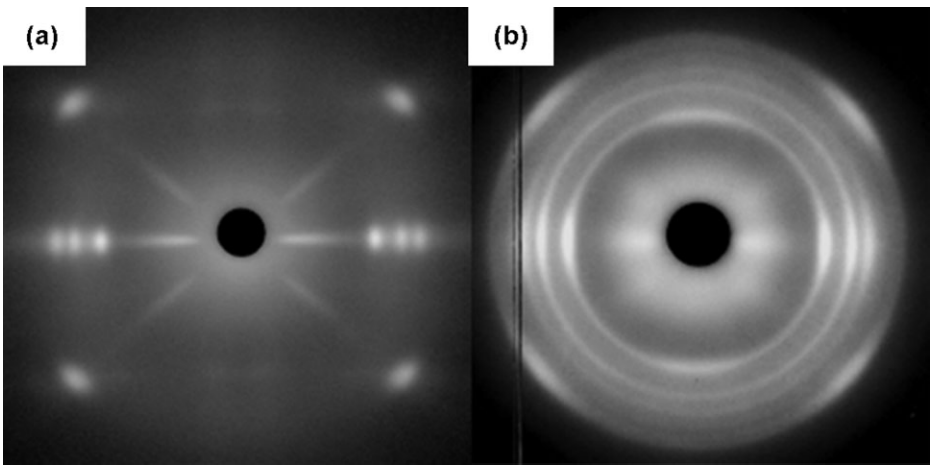

Figure 5 2D WAXS patterns of P/E17 stretched at 20°C: (a) In the stretched state; and (b) after recovery.

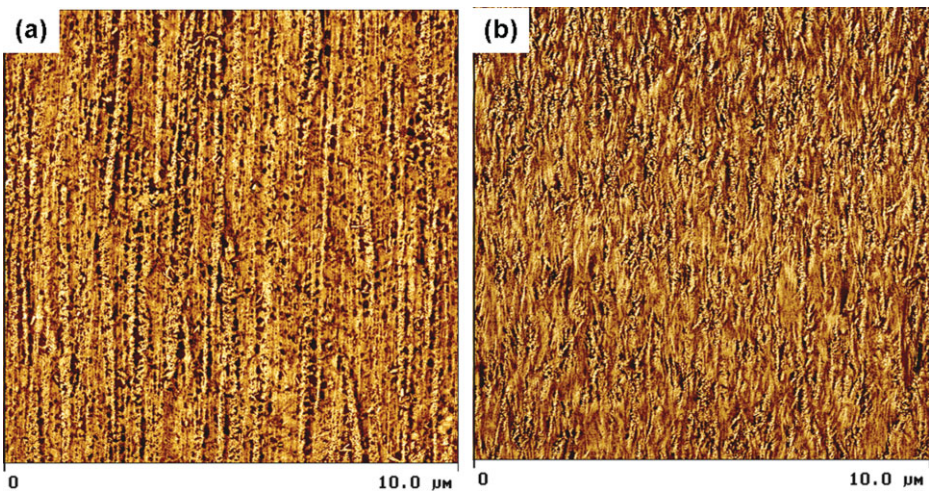

Figure 6 AFM images of P/E17 stretched at 20°C: (a) In the stretched state; and (b) after recovery. [Color figure can be viewed in the online issue, which is available at www.interscience.wiley.com.]

Figure 9. There was only a slight decrease from about 70 to 60% as the stretching temperature increased. The tensile modulus of the stretched specimens also decreased gradually as shown in Figure 10. The decreasing modulus presumably reflected the decreasing amount of crystalline phase that was available for orientation as the temperature increased.

The calculated fraction of γ-PP in the crystalline component of specimens drawn at the various temperatures and crystallized after strain recovery is given as the open symbols in Figure 11. Only the specimens drawn at 60 and 70°C contain a significant amount of the γ-form, although the content was lower than in the undeformed specimen. These data suggest that the γ-form of polypropylene is only nucleated in the recovered state when the specimen is cooled from above 50°C. It should be noted that the method used to obtain the amount of γ-PP, i.e., comparing the intensities of the two unique peaks (γ(117) and α(130)), failed for very small amounts of γ-PP because the γ(117) peak could not be distinguished from the amorphous halo in these cases. Therefore, the differences between specimens with γ-PP fraction of 0.1 or less may not be significant.

The 2D WAXS patterns from specimens stretched at 50°C and 70°C and crystallized after recovery are shown in Figure 12. The specimen drawn at 50°C showed much less crystalline phase orientation than the specimen drawn at ambient temperature, as indicated by the broader arcs in Figure 12(a) compared to Figure 5(b). The specimen drawn at 70°C had virtually no crystalline phase orientation, Figure 12(b),

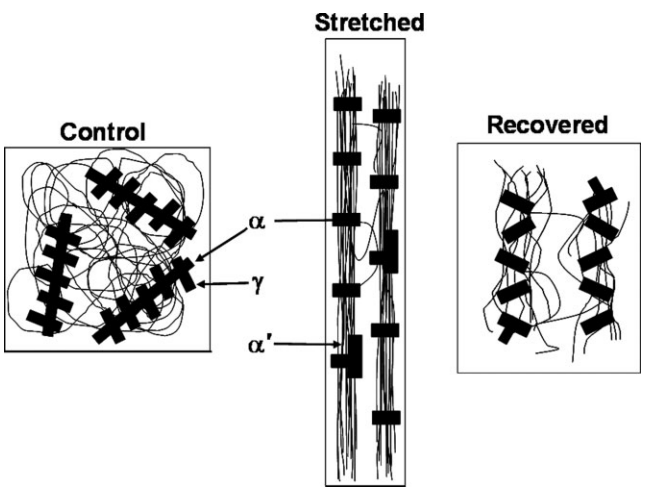

Figure 7 Structural model for the transformation of unoriented P/E17 to the stretched state at 600% elongation and after recovery from the stretched state.

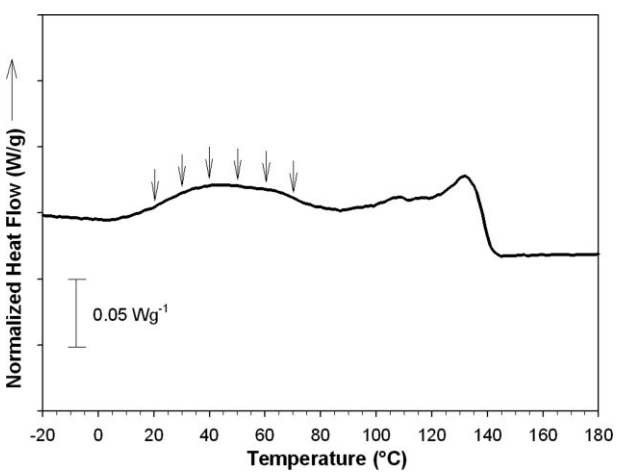

Figure 8 DSC melting thermogram of P/E17 indicating the temperatures of 20, 30, 40, 50, 60, and 70°C at which stretching was performed.

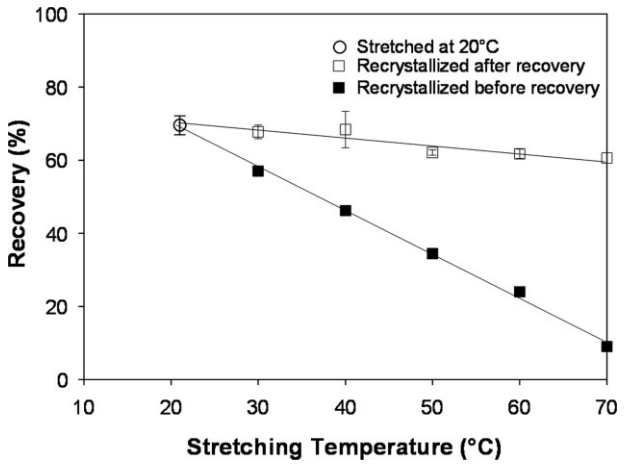

Figure 9 Effect of stretching temperature on the recovery after elongation to 600% for specimens recrystallized after and before recovery.

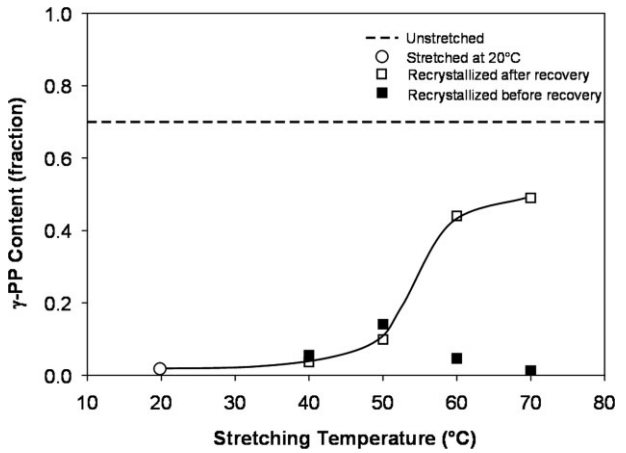

Figure 11 Effect of stretching temperature on the γ-PP content of specimens recrystallized after and before recovery from 600% elongation.

suggesting that the crystalline phase recrystallized isotropically after it recovered.

The WAXS of the recovered specimens indicated a population of α′-PP crystals. To determine the relative populations of the α-PP and α′-PP crystals, azimuthal scans were performed around the ring corresponding to the α(110) plane of selected specimens, Figure 13(a). The equatorial reflections are at 0° and 180°, whereas the broad meridional reflections are centered at 90° and 270°. The specimen stretched at 20°C showed high c-axis orientation of the α-PP phase with a small contribution from the α′-PP daughter lamellae. The crystalline phase in the specimen drawn at 50°C showed a smaller amount of orientation, whereas the one drawn at 70°C was virtually isotropic. The crystalline phase orientation was intrinsically related to the amorphous phase orientation. The decrease in modulus with increasing stretching temperature was probably the result of this decrease in orientation.

A description of the structural changes during deformation was developed, which is shown schematically in Figure 14. With increasing stretching temperature, a decreasing amount of crystalline material is available for orientation and fewer crystallites are available to act as physical crosslink junctions. This results in less orientation of the amorphous phase. On cooling, the melted portion of the polymer crystallizes isotropically, forming a network of isotropic crystals that is presumably connected by unoriented amorphous tie-chains. The specimen drawn at 70°C probably has slight amorphous phase orientation which is reflected by a slightly higher modulus than the unstretched specimen.

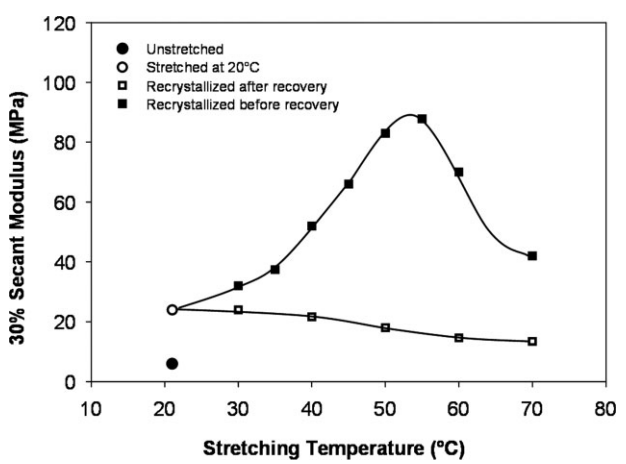

Figure 10 Effect of stretching temperature on the 30% secant modulus of specimens recrystallized after and before recovery from 600% elongation compared to unstretched PE/17.

Drawing at elevated temperatures with recrystallization before recovery

The order in which recrystallization and recovery were performed had a dramatic effect on the strain recovery and the modulus of the stretched films. The strain recovery for specimens crystallized before recovery, which is represented by the filled symbols in Figure 9, decreased linearly with increasing stretching temperature from 70% in specimens stretched at 20°C to less than 20% in specimens stretched at 70°C. The latter was in sharp contrast to the 60% strain recovery of the specimens stretched at 70°C but allowed to recover at the stretching temperature before recrystallization.

The tensile modulus of the stretched films is represented by the filled symbols in Figure 10. There was a sharp increase in modulus to a maximum value for specimens stretched at 55°C, followed by a sharp decrease in modulus for specimens stretched at higher temperatures. This contrasted with the monotonic

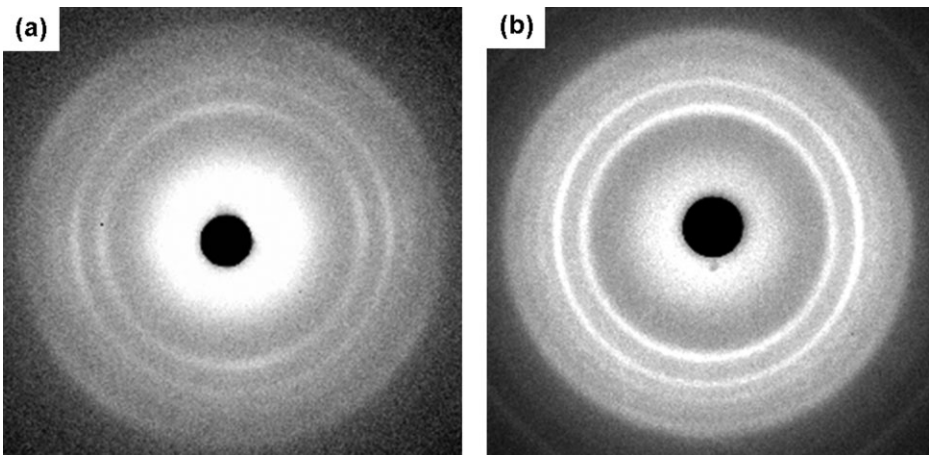

Figure 12 2D WAXS patterns of P/E17 stretched to 600% elongation at: (a) 50°C; and (b) 70°C, and recrystallized after recovery.

decrease in the modulus of specimens that were allowed to recover before they recrystallized.

The elasticity of the stretched films was measured in terms of the recovery from 30% strain based on the new gauge length. The recovery of two stretched films that differed substantially in the modulus is compared in Figure 15. The film stretched at 50°C and recrystallized before recovery had a modulus almost four times higher than the film stretched at 20°C. Nevertheless, both recovered over 90% almost instantaneously and recovered almost completely within 15 min. The high level of elasticity revealed that an elastomeric network persisted in both of the stretched films regardless of the stretching and recrystallization protocol. However, the manner in which the films were stretched and recrystallized did strongly affect the modulus.

The filled symbols in Figure 11 represent the fraction of γ-PP in the crystalline component of specimens drawn at the various temperatures and crystallized before recovery. All the specimens had predominantly the α-PP phase, even those stretched at the highest temperatures. In contrast to the specimens crystallized in the recovered state, these data suggest that the extended chains in P/E17 preferentially nucleated α-PP.

The 2D WAXS pattern in Figure 16(a) shows the high degree of orientation in a specimen drawn at 50°C and cooled in the stretched condition before recovery. In addition to the classic fiber pattern that was observed in the stretched condition for specimens drawn at 20°C [Fig. 5(a)], there were strong meridional reflections corresponding to α′-PP (110). Upon recovery, the specimen lost some orientation as is indicated by broadening of the equatorial spots into arcs in Figure 16(b). The 2D WAXS pattern captured in the stretched state for a specimen drawn at 70°C and recrystallized before recovery is shown in Figure 16(c). This pattern was very similar to that in Figure 16(a). However, the reflections from the α′-PP population were more intense. In contrast to the specimen that was drawn at 70°C and recrystallized after

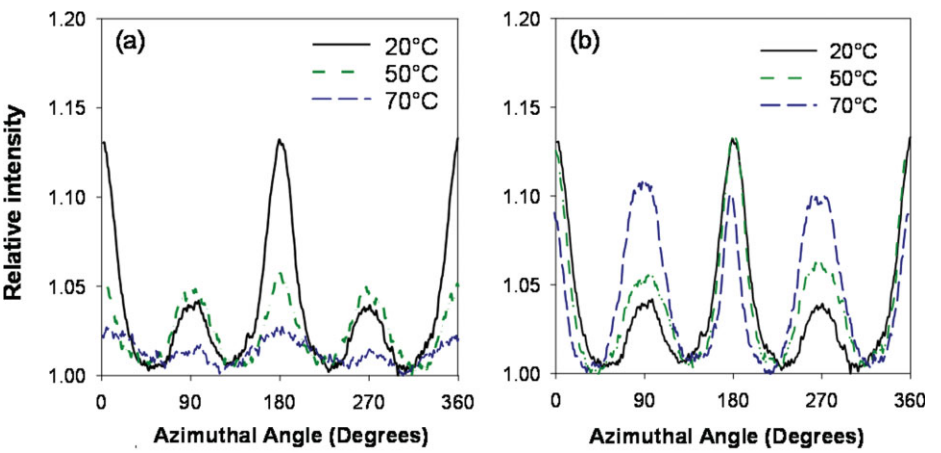

Figure 13 Azimuthal scans of the α110 reflections from 2D WAXS patterns for specimens stretched to 600% at various temperatures: (a) recrystallized after recovery; and (b) recrystallized before recovery. [Color figure can be viewed in the online issue, which is available at www.interscience.wiley.com.].

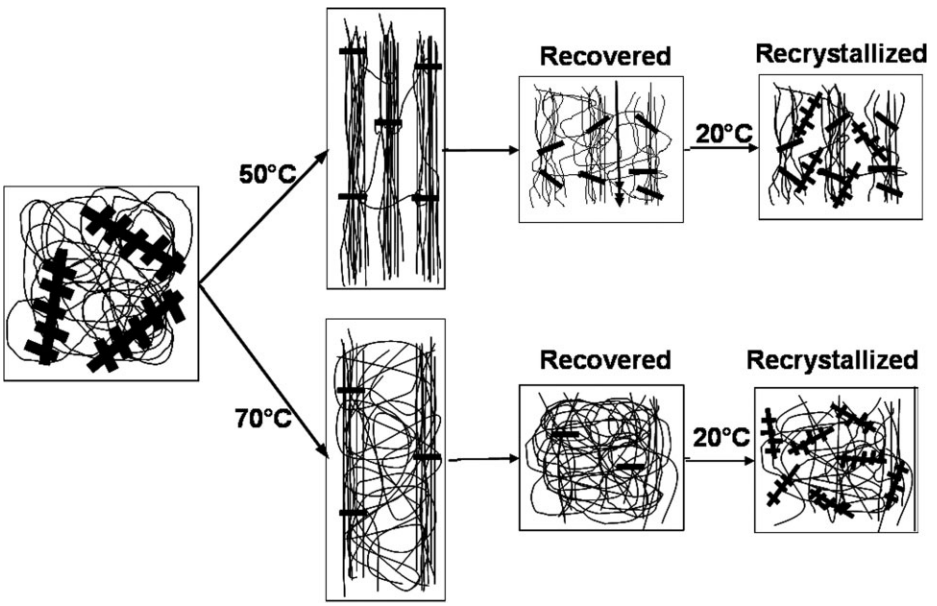

Figure 14 Structural models for specimens stretched to 600% at 50°C and 70°C and recrystallized after recovery.

recovery [Fig. 12(b)], the specimen recrystallized before recovery retained much higher crystal phase orientation in the recovered condition, Figure 16(d).

The azimuthal scans of specimens recrystallized before recovery are shown in Figure 13(b). For specimens drawn at 50 and 70°C, there was a large degree of crystalline phase orientation even after recovery. In addition, the amount of α′-PP daughter lamellae increased with increasing drawing temperature, which suggested that a large fraction of the melted polymer recrystallized epitaxially on the α-PP crystals during cooling. In contrast, the melted polymer recrystallized primarily as γ-PP when specimens stretched at the higher temperatures were allowed to recover before recrystallization.

The AFM of a specimen imaged in the stretched state after stretching at 50°C and cooling to ambient temperature is shown in Figure 17(a). Much like the specimen oriented at 20°C, there were well-defined fibrillar structures. However, the fibrils here were thinner and much more densely packed. After recovery, Figure 17(b), the specimen retained a larger degree of orientation compared to the specimen stretched at 20°C [Fig. 6(b)] as result of the lower strain recovery.

A structural model for specimens stretched at elevated temperature and recrystallized before recovery is shown in Figure 18. It is proposed that recrystallization in the stretched state results in the formation of a new molecular network with crystalline junction points formed before recovery. The new network prevents the strain recovery of the elongated chains to their entropically favored random coil state. The new network operates in opposition to the original network that formed from the unmelted crystal fraction during stretching. When the load is removed, contraction of the original network to its entropically favored state is opposed by compression of the newly formed network. The degree of strain recovery depends on the relative contributions of the two networks. It is suggested that the second network is anchored by the α′-PP daughter lamellae that crystallize epitaxially on the α-PP mother crystals of the extended fibers.

CONCLUSIONS

The effect of some process variables on the properties of a stretched propylene-ethylene elastomer was explored. Stretching at ambient temperature transformed the α-PP and γ-PP lamellar crystals into primarily α-PP shish-kebab fibers that acted as a scaffold for an elastomeric matrix of entangled, amorphous chains. Increasing the stretching temperature

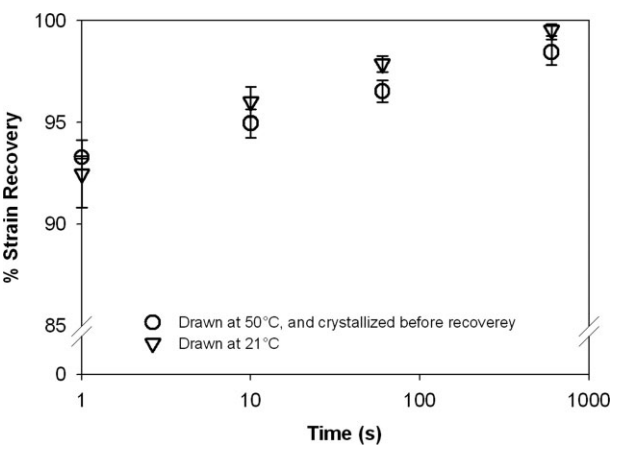

Figure 15 Recovery of stretched films from 30% strain.

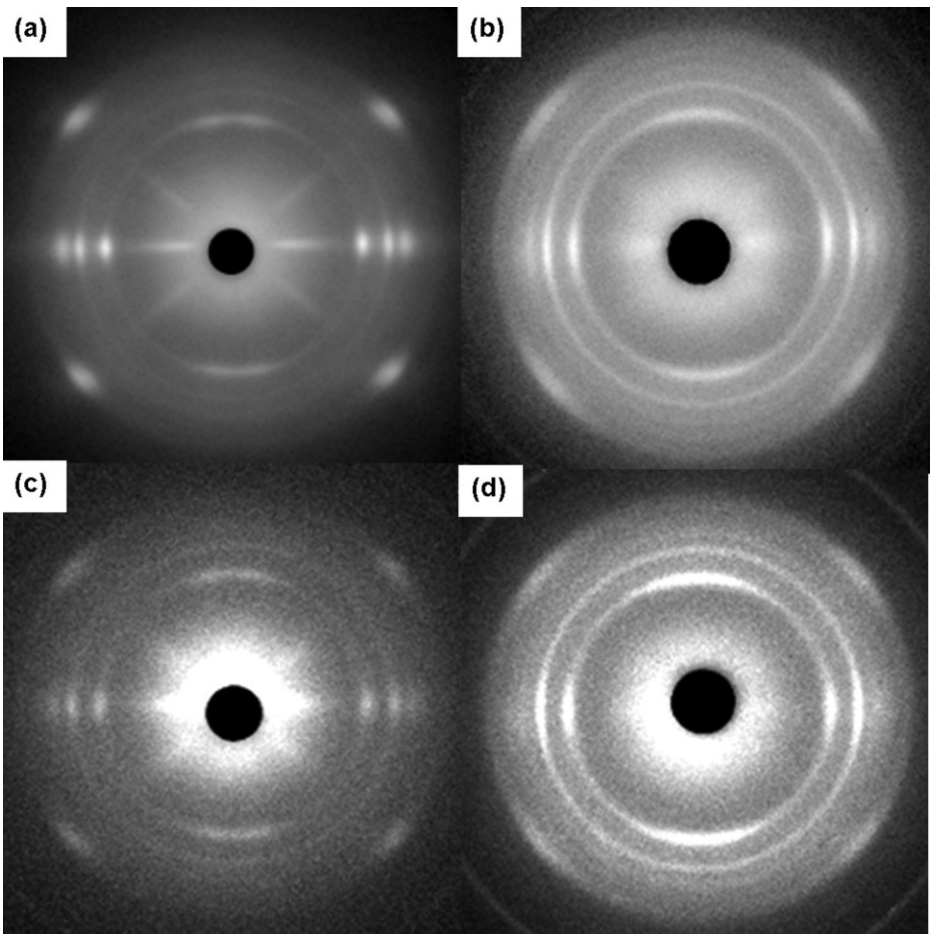

Figure 16 2D WAXS patterns of P/E17 stretched to 600%: (a) Stretched at 50°C and recrystallized by cooling to 20°C in the stretched state; (b) after recovery; (c) stretched at 70°C and recrystallized by cooling to 20°C in the stretched state; and (d) after recovery.

caused some of the crystals to melt and increased the amount of amorphous rubbery material in the film during stretching. Dramatic differences resulted depending on whether the stretched film was allowed to recover before or after recrystallization. Less recovery and substantially higher modulus

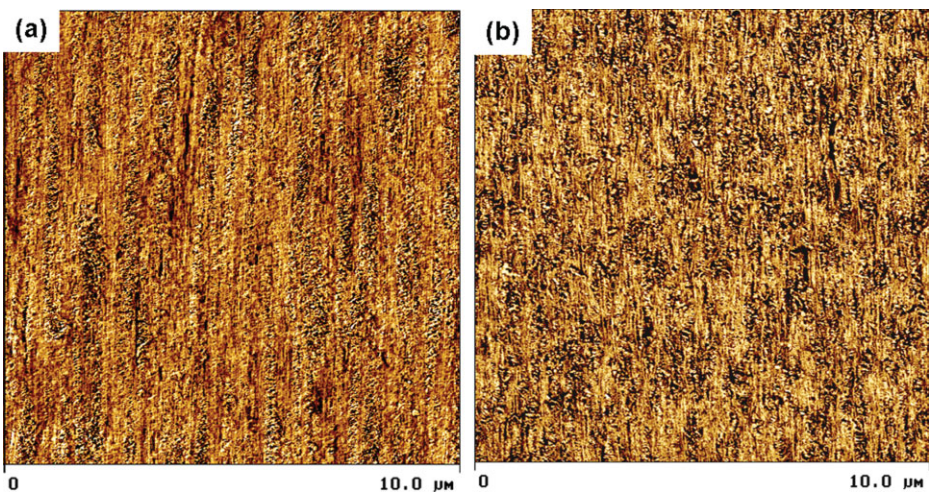

Figure 17 AFM images of P/E17: (a) Stretched at 50°C and recrystallized by cooling to 20°C in the stretched state; and (b) after recovery. [Color figure can be viewed in the online issue, which is available at www.interscience.wiley.com.]

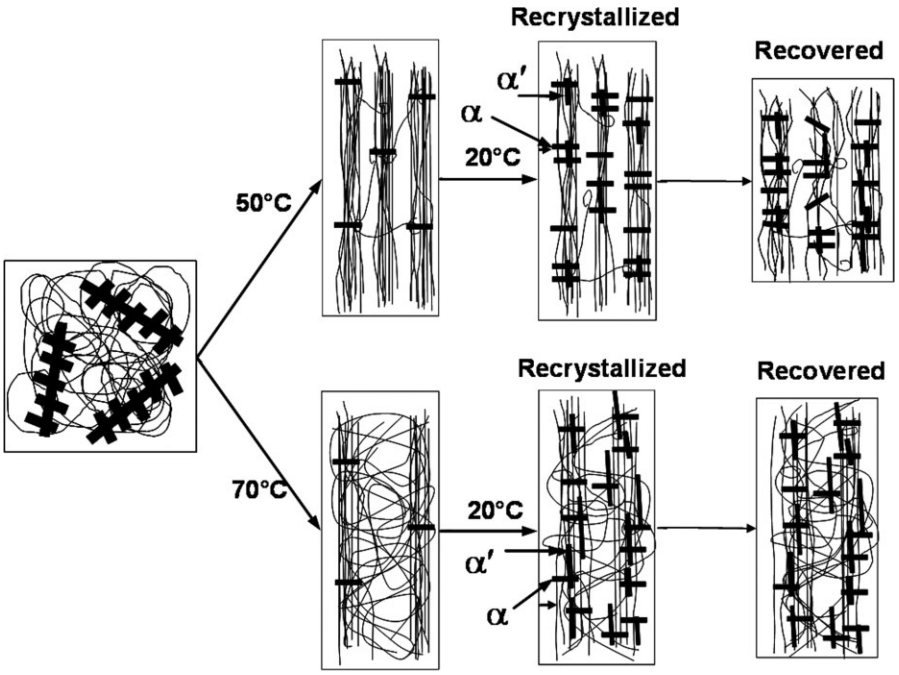

Figure 18 Structural models for specimens stretched to 600% at 50 and 70°C and recrystallized in the stretched state before recovery.

were obtained by allowing recrystallization before recovery. However, the high level of elasticity in the stretched films revealed that an elastomeric network persisted regardless of the stretching and recrystallization protocol.

Differences in the fibrous structure that formed during cooling and recrystallization were thought to be responsible for the observed properties. It is suggested that when recrystallization occurred in the stretched state, a second network formed that inhibited contraction of the oriented crystalline structure during strain recovery and froze the orientation of the stretched film. Stretching transformed the unmelted crystal fraction into fibers that subsequently provided the site for epitaxial recrystallization of the melted crystal fraction as α′-PP daughter lamellae. It is proposed that the α′-PP lamellae anchored the second network and operated in opposition to the fibrous α-PP network that formed during stretching. The good correlation between the fraction of α′-PP lamellae and the amount of residual strain indicated that that α′-PP lamellae played a key part in determining the final structure and properties of the stretched elastomer. It is possible that this concept can be extended to those processes that involve orientation of P/E copolymers in the melt or in the partially melted state, such as the spun bond fabric and elastic fiber processes. It may also serve as a guide for understanding the interrelationships among melting, processing temperatures, crystallization conditions, and the resulting properties of oriented products.

The authors thank Dr. Radoslaw Nowacki for valuable technical contributions, Dr. Dave Jarus from PolyOne for cryogrinding, and Mr. Joe Kolthammer for the strain recovery measurements.

References

1. Holden, G.; Legge, N. R.; Quirk, R. P.; Schroeder, H. E., Eds. Thermoplastic Elastomers, 2nd ed.; Hanser Publishers: New York, 1996, p 620.
2. Christenson, E. M.; Anderson, J. M.; Hiltner, A.; Baer, E. Polymer 2005, 46, 11744.
3. Bensason, S.; Minick, J.; Moet, A.; Chum, S.; Hiltner, A.; Baer, E. J Polym Sci Part B: Polym Phys 1996, 34, 1301.
4. Bensason, S.; Stepanov, E. V.; Chum, S.; Hiltner, A.; Baer, E. Macromolecules 1997, 30, 2436.
5. Stephens, C. H.; Poon, B. C.; Ansems, P.; Chum, S. P.; Hiltner, A.; Baer, E. J Appl Polym Sci 2006, 100, 1651.
6. Poon, B.; Rogunova, M.; Chum, S. P.; Hiltner, A.; Baer, E. J Polym Sci Part B: Polym Phys 2004, 42, 4357.
7. Dias, P.; Wang, H.; Nowacki, R.; Chang, A.; Van Dun, J.; Ansems, P.; Chum, S.; Hiltner, A.; Baer, E. In Proceedings of the Annual Technical Conference of Society of Plastics Engineers; Society of Plastics Engineers: Brookfield, CT, 2005, p 1227.
8. Poon, B. C.; Dias, P.; Ansems, P.; Chum, S. P.; Hiltner, A.; Baer, E. J Appl Polym Sci 2007, 104, 489.
9. Toki, S.; Sics, I.; Burger, C.; Fang, D.; Liu, L.; Hsiao, B. S.; Datta, S.; Tsou, A. H. Macromolecules 2006, 39, 3588.
10. Liu, L-Z.; Hsiao, B. S.; Fu, B. X.; Ran, S.; Toki, S.; Chu, B.; Tsou, A. H.; Agarwal, P. K. Macromolecules 2003, 36, 1920.
11. Samon, J. M.; Schultz, J. M.; Hsiao, B. S. Polymer 2002, 43, 1873.
12. Somani, R. H.; Hsiao, B. S.; Nogales, A.; Fruitwala, H.; Srinivas, S.; Tsou, A. H. Macromolecules 2001, 34, 5902.
13. Djiauw, L. K.; Gent, A. N. J Polym Sci Polym Symp 1974, 48, 159.
14. Brandrup, J.; Immergut, E. H. Polymer Handbook, 3rd ed.; Wiley: New York, 1989; Section V/27.

15. Isasi, J. R.; Mandelkern, L.; Galante, M. J.; Alamo, R. G. J Polym Sci Part B: Polym Phys 1999, 37, 323.
16. Olley, R. H.; Bassett, D. C. Polymer 1982, 23, 1707.
17. De Rosa, C.; Auriemma, F.; De Lucia, G.; Resconi, L. Polymer 2005, 46, 9461.
18. Lezak, E.; Bartczak, Z.; Galeski, A. Macromolecules 2006, 39, 4811.
19. Meille, S. V.; Bruckner, S.; Porzio, W. Macromolecules 1990, 23, 4114.
20. Turner-Jones, A.; Aizlewood, J. M.; Beckett, D. R. Makromol Chem 1964, 75, 134.
21. Turner-Jones, A. Polymer 1971, 12, 487.
22. Lotz, B.; Wittmann, J. C.; Lovinger, A. J. Polymer 1996, 37, 4979.
23. Dai, P. S.; Cebe, P.; Capel, M. J Polym Sci Part B: Polym Phys 2002, 40, 1644.
24. Alamo, R. G.; Ghosal, A.; Chatterjee, J.; Thompson, K. L. Polymer 2005, 46, 8774.
25. Dias, P.; Kazmierczak, T.; Ansems, P.; Chum, S.; Hiltner, A.; Baer, E. In Proceedings of the Annual Technical Conference of Society of Plastics Engineers; Society of Plastics Engineers: Brookfield, CT, 2007, p 1182.
26. Anderson, P. G.; Carr, S. H. J Mater Sci 1975, 10, 870.
27. Norton, D. R.; Keller, A. Polymer 1985, 26, 704.